A LIMIT CYCLE IN THE DYNAMICS OF A MAGNETIC VORTEX IN A TWO-DIMENSIONAL NANODOT

D.D. SHEKA, YU.B. GAIDIDEI[1], J.G. CAPUTO[2], J.P. ZAGORODNY[3], F.G. MERTENS[3]

UDC 537.61

Taras Shevchenko Kyiv National University
(64, Volodymyrska Str., Kyiv 01033, Ukraine; e-mail: denis_ sheka@univ.kiev.ua),

[1]**M.M. Bogolyubov Institute for Theoretical Physics, Nat. Acad. Sci. of Ukraine**
(14b, Metrolohichna Str, Kyiv 03143, Ukraine),

[2]**Laboratoire de Mathématiques, INSA de Rouen**
(B.P. 8, 76131 Mont-Saint-Aignan cedex, France)

[3]**Physics Institute, University of Bayreuth**
(95440 Bayreuth, Germany)

The dynamics of a magnetic vortex in a two-dimensional (2D) easy-plane ferromagnet under the influence of a magnetic field, which rotates in the magnet's plane, has been studied. Under such an influence, according to the results of numerical simulations, there appears a limit cycle in the magnetic vortex dynamics which exists in a wide range of field intensities and frequencies. Numerical results have been confirmed by analytical ones obtained in the framework of a new method of collective variables which takes into account both the internal degrees of freedom of the system and the coordinates of the vortex center.

1. Introduction

The study of various properties of magnetic vortices that exist in 2D magnets has been started since the middle of the 1980s. Today, we know well about the influence of vortices on the dynamic and thermodynamic properties of a magnet (see review [1]). In particular, vortices are responsible for the Berezinskii–Kosterlitz–Thouless topological phase transition [2–4]. The vortex contribution to the response functions of a ferromagnet has been calculated analytically [4] and confirmed experimentally [6]. Recently, the interest to the vortex dynamics has been renewed owing to the researches of magnetic nanodots – submicron-sized magnetic particles consisting of a magnetically soft material – where the vortex state can be the ground state due to a competition between the exchange and magnet-dipole interactions [7]. The researches of such nanodots are forward-looking now, because of their possible usage in high-density magnetic devices for the storage of information, high-rate elements of magnetic memory, and magnetic sensors [8, 9]. The vortex structure of nanodots has been observed experimentally with the help of Lorentz transmission electron microscopy [10,11] and magnetic force microscopy [12, 13]. The last two years have demonstrated the significant progress in experimental observations of the vortex properties of nanodots achieved thanks to Kerr microscopy with high time resolution [14], a phase sensitive Fourier transform imaging technique [15], and radiography [16].

Until recently, the macroscopic dynamics of vortices has been investigated in the framework of the standard Thiele equations [17–20], with the vortex being considered as a rigid particle-like excitation without any internal structure. However, the recent experimental [10, 21] and theoretical [22–27] studies testify to that there are phenomena which cannot be explained in the framework of the Thiele approach. In particular, the cycloidal oscillations of a vortex around its mean path [22,27] and the switching of magnetization at the vortex center [10, 21, 23–26] evidence for an essential coupling between the dynamics of the vortex center and spin waves.

The crucial role of the internal degrees of freedom in the dynamics of a vortex as a whole has been studied in

our previous work, where we have proposed the method of collective variables. In addition to the coordinates of the vortex center, this method also takes new variables into account which are responsible for the internal modes of the system.

In this work, we report in detail the results of our investigation of the problem concerning the vortex dynamics under the influence of an external field carried out making use of the data of numerical simulation and the new collective approach which takes the internal degrees of freedom into account. We show that an external ac field together with magnetic dissipation can stabilize the motion of a vortex in a confined circular spin system, which reproduces a magnetic nanodot. The properties of the limit cycle in the vortex dynamics were also studied. It has been shown that the vortex shape loses its radial symmetry. We have proposed a new ansatz which describes the limit dynamics of the vortex taking its symmetry into account. The method proposed can be considered as an extension of the Rice method of collective variables, the application of which for Klein—Gordon 1D kinks is well-known [28–30], onto the 2D case.

In Section 2, a discrete model is considered, a continual approach is formulated, and the structure of vortex-like solutions is discussed shortly. The results of numerical simulations of the vortex dynamics under the influence of the ac field are described in Section 3. The basic properties of the limit trajectory in the vortex dynamics are studied numerically. In Section 4, we propose and study in detail *a new method of collective variables* which describes the observable vortex dynamics and takes the internal degrees of freedom into account. The ways how to observe the described effects in real nanomagnets are discussed in Section 5.

2. Model, a Continual Description, and the Structure of Vortex-like Solutions

Consider a 2D uniaxial ferromagnet which is described by the following Hamiltonian:

$$\mathscr{H} = -\frac{J}{2}\sum_{(\boldsymbol{n},\boldsymbol{n}')} (\boldsymbol{S}_{\boldsymbol{n}}\boldsymbol{S}_{\boldsymbol{n}'} - \delta S^z_{\boldsymbol{n}} S^z_{\boldsymbol{n}'}) - \mathscr{V}(t)\,. \tag{1}$$

The first term is a classical Heisenberg Hamiltonian, where $\boldsymbol{S}_{\boldsymbol{n}} \equiv (S^x_{\boldsymbol{n}}, S^y_{\boldsymbol{n}}, S^z_{\boldsymbol{n}})$ is the classical spin with a fixed value S located at the point $\boldsymbol{n}$ of the 2D square lattice, and $J > 0$ is the exchange integral, with summation being carried on over all the nearest point pairs $(\boldsymbol{n}, \boldsymbol{n}')$. We assume that the anisotropy constant $\delta \in (0, 1)$ corresponds to the ground state of the easy-plane type. The influence of the uniform magnetic field $\boldsymbol{B}(t) = (B\cos\omega t, B\sin\omega t, 0)$, which rotates evenly in the plane of the magnet, is taken into account in the Hamiltonian through the additive Zeeman term $\mathscr{V}(t) = -\gamma B\sum_{\boldsymbol{n}} (S^x_{\boldsymbol{n}}\cos\omega t + S^y_{\boldsymbol{n}}\sin\omega t)$, where $\gamma = 2\mu_{\mathrm{B}}/\hbar$ is the gyromagnetic ratio.

A continual approximation for model (1) is valid in the case where the anisotropy constant $\delta \ll 1$ and the typical length of magnetic excitations $l_0 = a/\sqrt{4\delta}$ considerably exceeds the lattice constant a. In terms of angular variables

$$\boldsymbol{m} = \boldsymbol{S}/S = (\sin\theta\cos\phi; \sin\theta\sin\phi; \cos\theta)\,, \tag{2}$$

the functional of the total energy normalized by πJS^2 looks like

$$\mathscr{E}[\theta,\phi] = \frac{1}{2\pi}\int d^2\xi \Big[(\nabla\boldsymbol{\theta})^2 + \sin^2\theta\,(\nabla\boldsymbol{\phi})^2 + \\ + \cos^2\theta - 2b\sin\theta\cos(\phi - \nu\tau)\Big]. \tag{3}$$

Hereafter, for the notations to be simpler, the following dimensionless quantities are used: the coordinate $\boldsymbol{\xi} \equiv \boldsymbol{r}/l_0$, the time $\tau \equiv \omega_0 t$, the frequency $\nu = \omega/\omega_0$, and the amplitude $\boldsymbol{b} = \gamma\boldsymbol{B}/\omega_0$ of the external field [31, 32], where $\omega_0 = 4J\delta S$.

The dynamics of the system which corresponds to Eq. (3) is described by the Landau–Lifshits equation for the magnetization $\boldsymbol{m}$, taking the relaxation into account. These equations can be derived in the framework of the Lagrangian approach, starting from a Lagrangian in the form

$$\mathscr{L} = -\frac{1}{\pi}\int d^2\xi(1 - \cos\theta)\partial_\tau\phi - \mathscr{E}[\theta,\phi] \tag{4}$$

and the dissipation function

$$\mathscr{F}[\theta,\phi] = \frac{\varepsilon}{2\pi}\int d^2\xi\,(\partial_\tau\boldsymbol{m})^2 = \\ = \frac{\varepsilon}{2\pi}\int d^2\xi\,\Big[(\partial_\tau\theta)^2 + \sin^2\theta\,(\partial_\tau\phi)^2\Big]\,. \tag{5}$$

The Landau–Lifshits equations in terms of the variables θ and ϕ look like

$$\Delta\theta + \sin\theta\cos\theta\left[1 - (\boldsymbol{\nabla}\phi)^2\right] + b\cos\theta\cos(\phi - \nu\tau) =$$

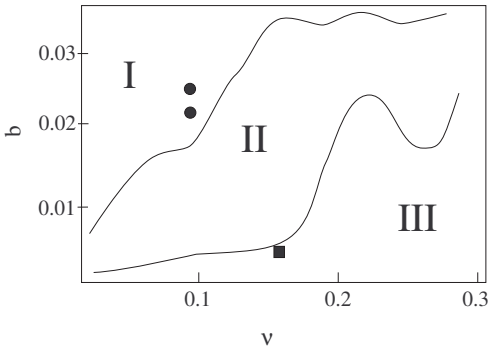

Fig. 1. Regions of the trajectories of different types in the plane of parameters (ν, b) in the range $\nu \in (0, 0.3)$ and $b \in (0, 0.033)$. The radius of the system $L = 36a \approx 20$. If the parameters are in region I, the vortex quits the system; if in region II, there is a limit cycle in the system; and if in region III, the vortex resides in the system for $\tau \lesssim 6400$, but limit cycles are not observed

$$= \sin\theta\partial_\tau\phi + \varepsilon\partial_\tau\theta, \tag{6a}$$

$$\boldsymbol{\nabla}\left(\sin^2\theta\boldsymbol{\nabla}\phi\right) - b\sin\theta\sin\left(\phi - \nu\tau\right) =$$

$$= -\sin\theta\partial_\tau\theta + \varepsilon\sin^2\theta\partial_\tau\phi. \tag{6b}$$

In the absence of a magnetic field, the ground state of the system is a uniform easy plane, $\theta_0 = \pi/2$, and $\phi = \text{const}$. The field changes the physical picture essentially: spins become evenly rotating in the plane, so that $\phi = \varphi + \nu\tau$. Such a precession results in the dynamic emergence of the z-component of magnetization ($\theta_0 \neq \pi/2$). Using Eqs. (6), one can easily estimate the equilibrium values of θ and ϕ. Supposing that $|\theta_0 - \pi/2| \ll 1$, we obtain

$$\cos\theta \approx \frac{\nu}{1-b}, \quad \phi = \nu\tau + \pi + \arcsin\frac{\varepsilon\nu}{b}. \tag{7}$$

An elementary nonlinear excitation of the system is an out-of-plane magnetic vortex [19, 20]. Let us consider its structure in the absence of an external magnetic field and the dissipation. For a circular system of radius L (in terms of l_0) and provided free (Neumann) boundary conditions, we have [27]

$$\theta = \theta\left(\rho\right), \quad \rho \equiv |z - Z|, \tag{8a}$$

$$\phi = q\arg\left(z - Z\right) - q\arg\left(z - Z_I\right) + q\arg Z, \tag{8b}$$

where $z = x + iy$ is the point on the XY-plane, $Z = X + iY = R\exp(i\Phi)$ is the coordinate of the vortex center, $q \in \mathbb{Z}$ is a π_1-topological charge of the vortex (the vorticity), the image of the vortex is located at the point $Z_I = ZL^2/R^2$ satisfying thus the Neumann boundary conditions. The function $\theta(\rho)$ is a solution of the following boundary-value problem [33]:

$$\frac{d^2\theta}{d\rho^2} + \frac{1}{\rho}\frac{d\theta}{d\rho} + \sin\theta\cos\theta\left(1 - \frac{q^2}{\rho^2}\right) = 0, \tag{9a}$$

$$\theta(0) = 0, \quad \theta(\infty) = \frac{\pi}{2}. \tag{9b}$$

Below, we consider only vortices with a unit topological charge ($q = 1$), because they possess the lowest energy.

3. Numerical Simulation of the Vortex Dynamics

To study the vortex dynamics under the influence of an external field that rotates in the magnet's plane, we modeled the evolution by the discrete Landau–Lifshits equations for model (1)

$$\frac{d\boldsymbol{S_n}}{dt} = -\left[\boldsymbol{S_n} \times \frac{\partial\mathscr{H}}{\partial\boldsymbol{S_n}}\right] - \frac{\varepsilon}{S}\left[\boldsymbol{S_n} \times \frac{d\boldsymbol{S_n}}{dt}\right]. \tag{10}$$

We integrated Eqs. (10) numerically over the square lattice of $(2L)^2$ in dimension, using the fourth-order Runge–Kutta method with the time step of 0.01. In all cases, the vortex was initially positioned near the center of the circular system; the field and relaxation were switched on adiabatically during the time of about 100. Further details of the simulation are described in work [26].

When carrying on the simulation, we assumed that $J = S = 1$. In all cases, the anisotropy constant was taken $\delta = 0.08$, which corresponded to the magnetic length $l_0 \approx 1.77a$. The system's sizes were changed within the range $20a < L < 100a$. For the further simplification, we also fixed the relaxation constant $\varepsilon = 0.01$ in Eq. (10) and varied the parameters b, ν, and L. Depending on the system parameters, we observed the vortex either annihilating itself by going beyond the system boundaries or remaining in the system forever. In the latter case, a limit cycle can emerge in the dynamics of the vortex. The typical trajectories of vortices which result in the limit cycle are presented in Fig. 1 of our previous work [34], where a vortex has been shown to

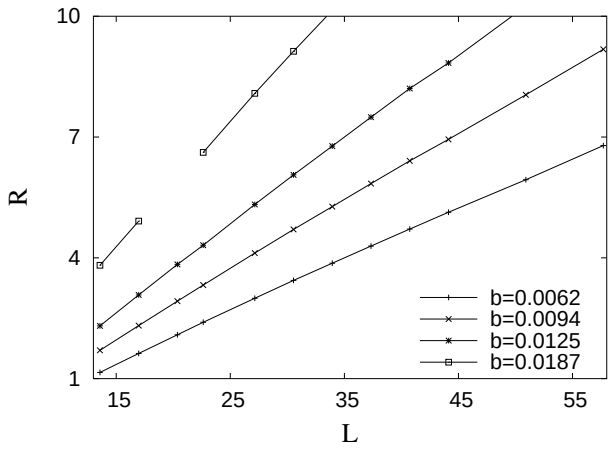

Fig. 2. Dependences of the vortex orbit radius R, provided the limit cycle is circular, on the system's size L at various field strengths b and for the fixed frequency of the field $\nu = 0.094$

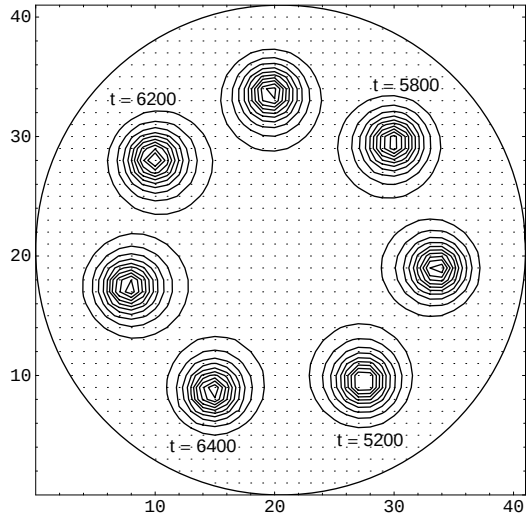

Fig. 3. Contour lines of the out-of-plane structures of the vortex in the absence of the field, at various times for the system with the radius $R = 20a$

move along the fixed limit trajectory, despite the initial conditions. The existence of the limit cycle requires both an external field and the dissipation in the system. Provided the fixed driving frequency ν and the given size L of the system, the limit cycle is absent if the field strength b is not strong enough. In this case, the dissipation processes dominate, which gives rise to the vortex annihilation, namely, the vortex quits the system moving along a spiral. In the opposite case, if the field strength b is very high in comparison with its frequency ν, the vortex also quits the system: the situation is similar to the vortex motion in an external quasistatic field which pushes the vortex out of a magnet. If both the parameters (the strength and the frequency) are very high, the field destroys the vortex forming spin waves.

In Fig. 1, the chart of different types of trajectories in the space of the parameters (ν, b) is presented for the system with the radius $L = 36a$. Note that there are "windows" in the chart for some parameter combinations, i.e. the events that were not expected for in those regions. For example, each circle designates the set of parameters, at which a trajectory of type III was observed in region I, and the square corresponds to the trajectory of type I in region III. We notice that an analogous situation was observed in work [26] while studying the phenomena of magnetization switching.

In the region, where the limit cycle is observed in the dynamics of the vortex, we numerically investigated the dependence of the vortex orbit radius R on the system size L. The plots of this dependence for various values of the field strength b are shown in Fig. 2. A linear dependence is observed in a wide interval of parameters $11 < L < 56$, with the observed frequency of motion along the limit trajectory Ω being lower than that of the field rotation ν.

4. Theoretical Description of the Vortex Dynamics in an AC Field

A conventional way to describe the collective dynamics of vortices is the method of Thiele equations [1]. In the framework of this method, the vortex is considered as a particle-like excitation which moves preserving its shape, according to the ansatz $\boldsymbol{m} = \boldsymbol{m}[z - Z(t)]$. Provided that the field is absent, this method adequately describes the observable circular motion of the vortex with the frequency [1]

$$\Omega(R) = \frac{1}{L^2 - R^2}. \tag{11}$$

In this case, the radius of the vortex orbit is defined by the initial conditions only. The hypothesis about the constant shape of a vortex in the absence of the field is confirmed by our simulation results (see Fig. 3). Namely, when moving along a circular trajectory, the vortex preserves its radially symmetric out-of-plane structure at every moment.

Consider now the vortex dynamics under the influence of the field. Calculations carried out in the framework of the Thiele approach showed that the vortex can move exclusively with the driving frequency.

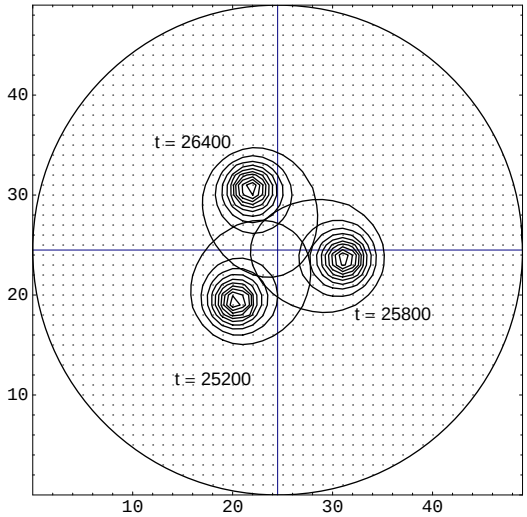

Fig. 4. Contour lines of the out-of-plane structures of the vortex in an external field with strength $b = 0.019$ and the frequency of rotation $\nu = 0.094$ at various times for the system with the radius $R = 24a$

Therefore, the results of numerical simulations, which were described in the previous section, cannot be explained in this way without taking into account the internal degrees of freedom.

The reason is that the magnetic field excites low-frequency quasi-Goldstone modes [23, 26] which can be connected with the translational mode of the vortex [25]. Thus, it is incorrect to describe the vortex as a rigid particle; instead, one must take into account its internal structure.

In the previous work [34], we proposed a new collective approach which takes into account not only the coordinates of the vortex center $\{R(\tau), \Phi(\tau)\}$ but also the "internal" variables $\{l(\tau), \Psi(\tau)\}$ on the basis of the ansatz

$$\theta(z,\tau) = \theta\left(\frac{|z - Z(\tau)|}{l(\tau)}\right), \tag{12a}$$

$$\phi(z,\tau) = \arg\Big(z - Z(\tau)\Big) - \arg\Big(z - Z_I(\tau)\Big) +$$

$$+ \arg Z(\tau) + \Psi(\tau) \tag{12b}$$

which describes a mobile vortex structure of type (8), but taking into account the precession of spins as a whole, due to the phase $\Psi(\tau)$, and the dynamics of the vortex core $l(\tau)$. The latter brings about the variation of the z-component of the total magnetization of the magnet.

We note that the out-of-plane structure of the vortex which is described by the variable θ is, according to Eq. (12a), radially symmetric with respect to the local position of the vortex center. Such a situation is typical in the absence of the field (see Fig. 3). However, the results of simulations evidence for the asymmetry of the out-of-plane structures of the vortex if the field does present (see Fig. 4). The contour lines $\theta = \text{const}$ are elliptically shaped and rotate together with the vortex preserving their form.

Thus, we suggest *a new asymmetric ansatz* which looks like

$$\theta(z,\tau) = \theta\left(\frac{|z - Z(\tau)|}{l(\tau,\alpha)}\right), \tag{13a}$$

$$\phi(z,\tau) = \alpha + \Phi(\tau) + \Psi(\tau), \tag{13b}$$

where the angle $\alpha = \arg(z - Z(\tau)) - \arg(z - Z_I(\tau))$ characterizes the polar angle with respect to the vortex center in the coordinate system that rotates together with the vortex (see Fig. 5). Under condition that the vortex is located at a distance $R \ll L$, the angular variable of the vortex image is almost constant, so that $\arg(z - Z_I(\tau)) \approx \Phi$. In this case, if one introduces the local polar coordinates

$$z - Z(t) = \rho \exp i\chi, \tag{14}$$

the angular variable $\alpha \approx \chi - \Phi$. We select the dependence $l(\tau,\alpha)$ in the form

$$l(\tau,\alpha) = \frac{1}{1 - A(t)\cos\alpha}. \tag{15}$$

This ensures the observable elliptic distortion of the vortex core (see Fig. 4) and corresponds to the excitation of an azimuthal mode, because, at $A \ll 1$, the oscillations of θ are approximately described by the dependence $\theta \approx \theta(\rho) + Af(\rho)\cos\alpha$ (cf. works [22, 35]). One should bear in mind that, everywhere throughout the text, we measure all the lengths in terms of l_0.

Asymmetric oscillations of the vortex core (15) are more beneficial energetically in comparison with uniform ones $l(\tau)$. The dynamic variable $A(\tau)$ is connected to the total number of bound magnons (or the number of spin deviations) in the system [33]:

$$N(\tau) = \frac{1}{\pi JS^2}\int d^2\xi\, \cos\theta(z,\tau) = \frac{N_0}{(1 - A^2)^{3/2}}. \tag{16}$$

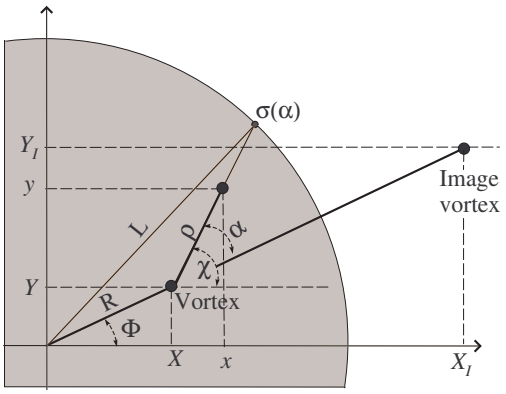

Fig. 5. The moving coordinate system centered at a moving vortex with the coordinate $Z = X + iY = R\exp(i\Phi)$

The quantity

$$N_0 = 2\int\limits_0^\infty \rho d\rho \cos\theta(\rho) \approx 2.75 \tag{17}$$

characterizes the number of magnons which are bound in a motionless vortex.

Note that, in the absence of pumping (the driving field) and dissipation, the quantity N is an integral of motion. The field excites the internal dynamics by changing the number of bound magnons N.

In order to derive the effective equations of motion, we use the variational method that was proposed by us in work [34]. Together with the "vortex" coordinates $\{R, \Phi\}$, we consider two "internal coordinates" $\{N, \Psi\}$; i.e. the system of collective variables is

$$X_i = \{R(\tau), \Phi(\tau), A(\tau), \Psi(\tau)\}\,. \tag{18}$$

For the effective Lagrangian to be constructed, we substitute the new ansatz (13) into total Lagrangian (4). The integration procedure is convenient to be carried out in the local coordinate system (14), taking into account the relationships

$$\int\limits_{|z|<L} f(\rho,\alpha)d^2\xi = \big\langle F(\alpha)\big\rangle, \quad F(\alpha) = 2\pi\int\limits_0^{\sigma(\alpha)} f(\rho,\alpha)\rho d\rho,$$

where $\sigma(\alpha)$ (see Fig. 5) is determined by the cosine theorem

$$\sigma(\alpha) = -R\cos\alpha + \sqrt{L^2 - R^2\sin^2\alpha}, \tag{19}$$

and the averaging is fulfilled according to the rule $\langle F(\alpha)\rangle = \frac{1}{2\pi}\int_0^{2\pi} F(\alpha)d\alpha$. In the main approximation

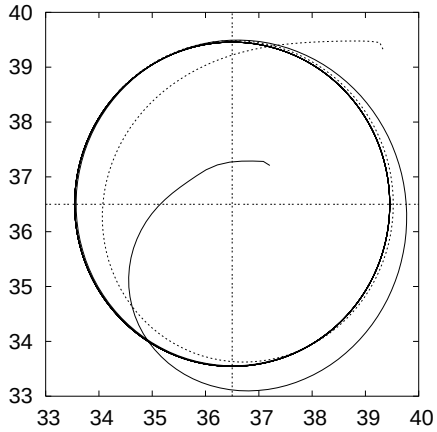

Fig. 6. Two trajectories of the vortex obtained by the numerical integration of the effective equations under various initial conditions: $R(0) = a$ (bold curve), $4a$ (dashed curve). The other parameters are $\Phi(0) = \pi/4$, $\Psi(0) = \pi/2$, $A_0 = 0.5$ $b = 0.01$, $\nu = 0.0625$, $\varepsilon = 0.01$, and $\delta = 0.08$. The radius of the system $L = 36a \approx 20$

and provided that $R/L \ll 1$, the expression for the derivative $\partial_\tau\phi$ in the moving coordinate system looks like

$$\partial_\tau\phi = \frac{\dot R}{\rho}\sin\alpha - \frac{R\dot\Phi}{\rho}\cos\alpha, \tag{20}$$

where the point designates the derivative $d/d\tau$.

The gyroscopic term $\mathscr{G}$ in the Lagrangian looks like

$$\mathscr{G} = \mathscr{G}_1 + \mathscr{G}_2,$$

$$\mathscr{G}_1 = -\frac{1}{\pi}\int d^2\xi\partial_\tau\phi = -2\dot R\Big\langle[\sigma(\alpha) - L/3]\sin\alpha\Big\rangle +$$

$$+2R\dot\Phi\Big\langle[\sigma(\alpha) - L/3]\cos\alpha\Big\rangle,$$

$$\mathscr{G}_2 = \frac{1}{\pi}\int d^2\xi\cos\theta\partial_\tau\phi = N\dot\Psi +$$

$$+k_0\dot R\big\langle l(\tau,\alpha)\sin\alpha\big\rangle - k_0R\dot\Phi\big\langle l(\tau,\alpha)\cos\alpha\big\rangle,$$

where the constant $k_0 = 2\int_0^\infty \cos\theta(\rho)d\rho \approx 2.676$. After the procedure of averaging with regard for the relationships

$$\Big\langle\sigma(\alpha)\cos\alpha\Big\rangle = -\frac{R}{2},\ \Big\langle\sigma(\alpha)\sin\alpha\Big\rangle = \Big\langle l(\tau,\alpha)\sin\alpha\Big\rangle = 0,$$

$$\left\langle l(\tau,\alpha)\cos\alpha\right\rangle = \frac{1}{A}\left(\frac{1}{\sqrt{1-A^2}}-1\right), \tag{21}$$

we ultimately obtain the gyroscopic term in the form

$$\mathscr{G} = N\dot{\Psi} - R^2\dot{\Phi} - \frac{k_0 R\dot{\Phi}}{A}\left(\frac{1}{\sqrt{1-A^2}}-1\right). \tag{22}$$

Let us proceed to the calculation of the functional of the total energy (3). We rewrite the energy in the form $\mathscr{E} = \mathscr{E}_1 + \mathscr{E}_2 + \mathscr{E}_3 + V$, where

$$\mathscr{E}_1 = \frac{1}{2\pi}\int d^2\xi(\boldsymbol{\nabla}\theta)^2 = \text{const}, \tag{23a}$$

$$\mathscr{E}_2 = \frac{1}{2\pi}\int d^2\xi \sin^2\theta(\boldsymbol{\nabla}\phi)^2 \approx \left\langle \ln\frac{L^2-R^2}{Ll(\tau,\alpha)}\right\rangle, \tag{23b}$$

$$\mathscr{E}_3 = \frac{1}{2\pi}\int d^2\xi\cos^2\theta = \frac{N}{2N_0}. \tag{23c}$$

$$\mathscr{V} = -\frac{b}{\pi}\int d^2\xi \sin\theta\cos(\phi-\nu\tau) \approx bRL\cos\Delta, \tag{23d}$$

$$\Delta = \Phi + \Psi - \nu\tau. \tag{24}$$

The interaction of the vortex with its image, which is described by the term $\mathscr{E}_2$, can be found making use of the results of calculations carried out in the case of the zero field which were presented in work [27],

$$\mathscr{E}^{\text{int}} = \mathscr{E}_0 + \pi\ln\frac{L^2-R^2}{Ll_0}, \tag{25}$$

by substituting $l(\tau)$ for l_0. While calculating the last anisotropic term $\mathscr{E}_3$, we used the relationship $\int_0^\infty \cos\theta^2(\rho)\rho d\rho = 1/2$ (see work [31]).

Ultimately, the effective Lagrangian can be written down as follows:

$$\mathscr{L} = \frac{N_0\dot{\Psi}-1/2}{(1-A^2)^{3/2}} - R^2\dot{\Phi} - \frac{k_0 R\dot{\Phi}}{A}\left(\frac{1}{\sqrt{1-A^2}}-1\right) -$$

$$-\ln\left[\frac{A^2(L^2-R^2)}{2L\left(1-\sqrt{1-A^2}\right)}\right] - bLR\cos\Delta. \tag{26}$$

The effective dissipation function can be calculated in a similar way, by substituting ansatz (13) into the microscopic dissipation function (5)

$$\mathscr{F} \approx \frac{\varepsilon}{2}\left[\left(\dot{R}^2 + R^2\dot{\Phi}^2\right)\ln L + L^2\dot{\Psi}^2 + 2R^2\dot{\Phi}\dot{\Psi} + \right.$$

$$\left. + C_1\dot{R}\dot{A} + C_2\left(\dot{A}^2 + A^2\dot{\Phi}^2\right)\right], \tag{27}$$

where the constants C_1 and C_2 are defined as

$$C_1 = 2\int_0^\infty \theta'^2\rho^2 d\rho \approx 1.372,$$

$$C_2 = \int_0^\infty \theta'^2\rho^3 d\rho \approx 0.962.$$

The effective equations of motion can be derived as ordinary Euler—Lagrange equations

$$\frac{\partial\mathscr{L}}{\partial X_i} - \frac{d}{d\tau}\left(\frac{\partial\mathscr{L}}{\partial\dot{X}_i}\right) = \frac{\partial\mathscr{F}}{\partial\dot{X}_i} \tag{28}$$

for the system of collective variables (18), using Lagrangian (26) and the dissipation function (27).

The full system of effective equations is rather cumbersome. Therefore, below, we present its simplified version only. For the numerical integration of the system of effective equations (28), one has to solve a linear system at every step. For this purpose, we used MAPLE software [36] which provides necessary capabilities. The numerical analysis testifies to that the system of effective equations describes the principal properties of the observed dynamics and reveals the existence of the limit cycle for the vortex trajectory (see Fig. 7). We notice that the coupling between the vortex coordinates and the "internal coordinates" $\{A, \Psi\}$ is necessary for the limit cycle to exist.

The effective model provides the existence of trajectories of various types (see Fig. 7). Vortex trajectories compose the limit cycle only at $b \lesssim \nu/2$ (region II). If the strength of the magnetic field is higher than the indicated critical value, the vortex annihilates itself, by quitting the system (range I). The model does not imply the lower limiting value for the availability of the limit cycle. But, in Fig. 7, the dashed line denotes a curve which satisfies a condition, under which the orbit radius can become smaller than the lattice constant (region III). In this case, the effects of discreteness come into action, so that the model ceases to be adequate.

In Fig. 8, the dependences of the vortex orbit radius on the system size are shown. They were obtained by the numerical integration of the system of effective equations. We note that the linear dependence $R \propto L$

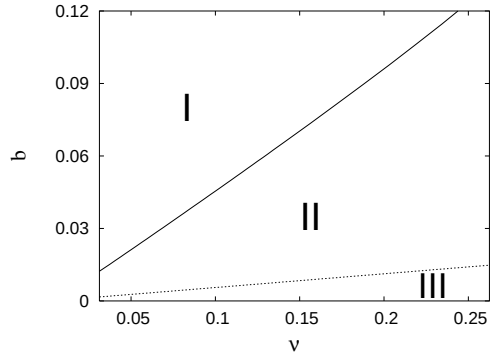

Fig. 7. Three regions corresponding to trajectories of different types in the plane of parameters (ν, b) calculated by the numerical integration of the effective equations. The parameters of the system are $\varepsilon = 0.01$ and $\delta = 0.08$. The size of the system $L = 36a \approx 20$

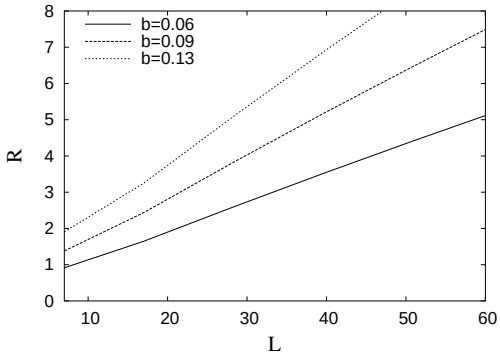

Fig. 8. Dependences of the vortex orbit radius R, provided the limit cycle is circular, on the system's size L, obtained by the numerical integration of the effective equations, at various field strengths b and for the fixed frequency of the field $\nu = 0.06$. The other parameters coincide with those in Fig. 2

is similar to the dependence that was obtained by the numerical simulation (cf. Fig. 2).

For analyzing the model analytically, we make some simplifications which are confirmed by the results of simulations. First, we assume the vortex to be always far from the boundary, i.e. $R \ll L$. Secondly, we suppose the degree of elliptic distortion of the vortex core to be very small, i.e. $A \ll 1$. Provided those assumptions, the Lagrangian of system (26) and the dissipation function (27) acquire the forms

$$\mathscr{L} = \frac{A^2}{2}\left(3N_0\dot{\Psi} - 1\right) - R^2\dot{\Phi} + \frac{R^2}{L^2} -$$

$$-\frac{k_0 RA\dot{\Phi}}{2} - bRL\cos\Delta, \tag{29a}$$

$$\mathscr{F} = \eta\left(\dot{R}^2 + R^2\dot{\Phi}^2\right) + \varepsilon\frac{L^2}{2}\dot{\Psi}^2 + \varepsilon R^2\dot{\Phi}\dot{\Psi}, \tag{29b}$$

where $\Delta \equiv \Phi + \Psi - \nu\tau$ and the dissipation constant $\eta = (\varepsilon/2)\ln L$.

Making use of Eqs. (29), we calculate the effective equations which have rather a simple form:

$$\left(1 + \frac{k_0 A}{4R}\right)\dot{R} = \eta R\dot{\Phi} - \frac{bL}{2}\sin\Delta + \varepsilon\frac{R}{2}\dot{\Psi} - \frac{k_0\dot{A}}{4}, \tag{30a}$$

$$\left(1 + \frac{k_0 A}{4R}\right)\dot{\Phi} = \frac{1}{L^2} - \eta\frac{\dot{R}}{R} - \frac{bL}{2R}\cos\Delta, \tag{30b}$$

$$3N_0 A\dot{A} = -\varepsilon L^2\dot{\Psi} + bRL\sin\Delta - \varepsilon R^2\dot{\Phi}, \tag{30c}$$

$$3N_0\dot{\Psi} = 1 + \frac{k_0 R\dot{\Phi}}{2A}, \tag{30d}$$

The system of equations (30) describes two damped coupled oscillators with a periodic pumping and includes two pairs of arguments, (R, Φ) and (A, Ψ). Under the influence of the pumping, the oscillators can synchronize each other and form a limit cycle which is characterized by the conditions

$$\dot{R} = \dot{A} = 0, \qquad \dot{\Phi} \equiv \Omega = \text{const}, \quad \dot{\Psi} = \nu - \Omega. \tag{31}$$

As a result, we obtain the following system of three algebraic equations

$$\varepsilon R(\nu + C\Omega) = bL\sin\Delta, \tag{32a}$$

$$\varepsilon L(\nu - \Omega) = bR\sin\Delta, \tag{32b}$$

$$-\left(2R + \frac{k_0 A}{2}\right)\Omega = bL\cos\Delta, \tag{32c}$$

where $C = \ln L - 1$. Excluding $\sin\Delta$ from the first two equations, we obtain the expression for the frequency of the vortex motion,

$$\Omega \approx \frac{\nu}{1 + CR^2/L^2}. \tag{33}$$

Then, from relations (32a) and (32c), we get $R \approx bL/2\Omega$. Combining the latter with Eq. (33), we obtain

$$\Omega \approx \frac{\nu + \sqrt{\nu^2 - Cb^2}}{2}. \tag{34}$$

The value of the frequency of the vortex motion Ω is lower than the field frequency ν, in accordance with the results of the simulation. Ultimately, for the radius of the limit cycle, we have

$$R \approx \frac{bL}{\nu + \sqrt{\nu^2 - Cb^2}} \approx \frac{bL}{2\nu}. \tag{35}$$

The linear dependence $R \propto L$ was observed in the simulation (see Fig. 2).

We note that, according to Eq. (35), the radius of the limit cycle R becomes real if the additional condition $\nu^2 - Cb^2 > 0$ holds true. This relationship predetermines the natural limit for the limit cycle to exist. The other limit of the existence is connected to the effects of discreteness, $Rl_0 > a$. Thus, the range where the limit cycle exists is determined by the relation

$$\frac{b}{\nu} \in \left(\frac{2a}{l_0 L}; \frac{1}{\sqrt{\ln L - 1}} \right). \tag{36}$$

5. Conclusions

To summarize, we have developed a new method of collective variables to describe the dynamics of vortices under the influence of a periodic magnetic field taking into account the internal degrees of freedom of the system. As far as we know, it is the first attempt to show that the interaction between the internal and external degrees of freedom in 2D magnetic systems can result in the appearance of stable trajectories. A new ansatz describes, with an accuracy to a factor of about 2, the radius of the limit cycle and allows one to obtain a correct functional dependence $R \propto bL/\nu$. However, the analytic expression for the frequency of vortex rotation $\Omega \lesssim \nu$ (34) does not correspond to the result of the simulation, which evidence for $\Omega \ll \nu$. Despite this circumstance, we hope that the new method of collective variables has a rather general character and can be applied to the self-consistent description of the dynamics of 2D nonlinear excitations, in particular, topological solitons in 2D easy-plane magnets [37].

The researches carried out in the work are of practical importance in nanomagnetism. Vortices are known to be responsible for hysteretic properties in magnetic nanostructures if the characteristic size of a nanoparticle exceeds the radius of the domain [8]. Usually, experimentally studied are the static hysteretic properties, i.e. the dependence $M_x(H_x)$ is measured (see works [11,13,38,39]). The saturation field is of the order of ω_0/γ ($b \sim 1$, in dimensionless units) in such a static regime. In this work, we have considered the dynamical properties of vortices under the influence of an ac field which causes the dynamical hysteresis, $M_x(b)$. Typical values of the saturation field, i.e. the field, at which the vortex annihilates itself by quitting the system, are easy to be estimated on the basis of relationship (36). Typical values of the annihilation field, $b \sim \nu/\sqrt{\ln L - 1} \ll 1$, are considerably lower than for the static mode. Let us make some estimations. For a nanodot fabricated of permalloy (Py, $Ni_{80}Fe_{20}$) [11, 38], the saturation magnetization $M_s = \gamma SL^2/a^2 = 770$ G, the exchange constant $A = JS^2 = 1.3 \times 10^{-6}$ erg/cm, and $\gamma/2\pi = 2.95$ GHz/kOe [14]. Therefore, typical fields of vortex annihilation $b \sim \nu/\sqrt{\ln L - 1}$ are of the order of tens of oersteds. Other important information is connected with the fact that the vortex state becomes unstable in a very small system. According to the earlier simulation data, the minimal characteristic size of the system $L_{\min} \sim 5$. For a permalloy nanodot, a typical magnetic length (the so-called exchange length) $l_0 = 5.9$ nm [14], so that the size of a nanodot in the vortex state and subjected to a weak ac pumping $L_{\min} l_0 \sim 30$ nm. This means that the vortex state in a nanodot with diameter more than 60 nm is unstable with respect to a periodic field, which results in the vortex annihilation and the appearance of a single-domain state.

D.D. Sheka and Yu.B. Gaididei were supported by the joint Ukrainian-German project "Engineered nonlinear excitations in magnetic nanostructures" (DLR grant No. UKR-02-011 and grant of the Ministry of Education and Science of Ukraine No. M/82-2004), by the joint Ukrainian-French project "Dnipro" (EGIDE grant No. 09855 and grant of the Ministry of Education and Science of Ukraine No. M/80-2005). The work of D.D. Sheka was patially supported by the Ukrainian-Indian project (grant of the Ministry of Education and Science of Ukraine No. M/270-2004).

1. *Mertens F.G., Bishop A.R.* // Nonlinear Science at the Dawn of the 21th Century / Ed. by P.L. Christiansen, M.P. Soerensen, Scott A.C. — Berlin: Springer, 2000.
2. *Berezinskii V.L.* // Sov. Phys. JETP. — 1972. — **34**. — P. 610.
3. *Kosterlitz J. M., Thouless D.J.* // J. Phys. C. — 1973. — **6**. — P. 1181.
4. *Kosterlitz J. M.* // Ibid. — 1974. — **7**. — P. 1046.
5. *Mertens F.G., Bishop A.R., Wysin G.M., Kawabata C.* // Phys. Rev. B. — 1989. — **39**. — P. 591.
6. *Wiesler D.D., Zabel H., Shapiro S.M.* // Physica B. — 1989. — **156—157**. — P. 292.
7. *Hubert A., Schäfer R.* Magnetic Domains. — Berlin: Springer, 1998.

8. *Cowburn R.P.* // J. Magn. and Magn. Mater. — 2002. — **242—245**. — P. 505.
9. *Skomski R.* // J. Phys. C. — 2003. — **15**. — P. R841.
10. *Raabe J., Pulwey R., Sattler R. et al.* // J. Appl. Phys. — 2000. — **88**. — P. 4437.
11. *Schneider M., Hoffmann H., Otto S. et al.* // Ibid. — 2002. — **92**. — P. 1466.
12. *Pokhil T., Song D., Nowak J.* // Ibid. — 2000. — **87**. — P. 6319.
13. *Fernandez A., Cerjan C.J.* // Ibid. — P. 1395.
14. *Park J.P., Eames P., Engebretson D.M. et al.* // Phys. Rev. B. — 2003. — **67**. — P. 020403(R)
15. *Buess M., Höllinger R., Haug T. et al.* // Phys. Rev. Lett. — 2004. — **93**. — P. 077207.
16. *Choe S.B., Acremann Y., Scholl A. et al.* // Science. — 2004. — **304**. — P. 420.
17. *Thiele A.A.* // Phys. Rev. Lett. — 1973. — **30**. — P. 230.
18. *Thiele A.A.* // J. Appl. Phys. — 1974. — **45**. — P. 377.
19. *Huber D.L.* // Phys. Rev. B. — 1982. — **26**. — P. 3758.
20. *Nikiforov A.V., Sonin É.B.* // Sov. Phys. JETP. — 1983. — **58**. — P. 373.
21. *Pulwey R., Rahm M., Biberger J., Weiss D.* // IEEE Trans. on Magnetics. — 2001. — **37**. — P. 2076.
22. *Ivanov B.A., Schnitzer H.J., Mertens F.G., Wysin G.M.* // Phys. Rev. B. — 1998. — **58**. — P. 8464.
23. *Gaididei Y., Kamppeter T., Mertens F.G., Bishop A.R.* // Ibid. — 2000. — **61**. — P. 9449.
24. *Kovalev A.S., Prilepsky J.E.* // Low Temp. Phys. — 2002. — **28**. — P. 921.
25. *Kovalev A.S., Prilepsky J.E.* // Ibid. — 2003. — **29**. — P. 55.
26. *Zagorodny J.P., Gaididei Y., Mertens F.G., Bishop A.R.* // Eur. Phys. J. B. — 2003. — **31**. — P. 471.
27. *Kovalev A.S., Mertens F.G., Schnitzer H.J.* // Ibid. — **33**. — P. 133.
28. *Rice M.J.* // Phys. Rev. B. — 1983. — **28**. — P. 3587.
29. *Quintero N.R., Sanchez A., Mertens F.G.* // Phys. Rev. Lett. — 2000. — **84**. — P. 871.
30. *Quintero N.R., Sanchez A., Mertens F.G.* // Phys. Rev. E. — 2000. — **62**. — P. 5695.
31. *Ivanov B.A., Sheka D.D.* // Low Temp. Phys. — 1995. — **21**. — P. 1148.
32. *Ivanov B.A., Wysin G.M.* // Phys. Rev. B. — 2002. — **65**. — P. 134434.
33. *Kosevich A.M., Ivanov B.A., Kovalev A.S.* // Phys. Repts. — 1990. — **194**. — P. 117.
34. *Zagorodny J.P., Gaididei Y., Sheka D.D. et al.* // Phys. Rev. Lett. — 2004. — **93**. — P. 167201.
35. *Sheka D.D., Yastremsky I.A., Ivanov B.A. et al.* // Phys. Rev. B. — 2004. — **69**. — P. 054429.
36. URL http://www.maplesoft.com.
37. *Sheka D.D., Ivanov B.A., Mertens F.G.* // Phys. Rev. B. — 2001. — **64**. — P. 024432.
38. *Cowburn R.P., Koltsov D.K., Adeyeye A.O. et al.* // Phys. Rev. Lett. — 1999. — **83**. — P. 1042.
39. *Lebib A., Li S.P., Natali M., Chen Y.* // J. Appl. Phys. — 2001. — **89**. — P. 3892.

Received 19.01.05.
Translated from Ukrainian by O.I. Voitenko

ГРАНИЧНИЙ ЦИКЛ В ДИНАМІЦІ МАГНІТНОГО ВИХОРУ У ДВОВИМІРНІЙ НАНОТОЧЦІ

Д.Д. Шека, Ю.Б. Гайдідей, Ж.Г. Капуто, Х.П. Загороднiй, Ф.Г. Мертенс

Р е з ю м е

Досліджено динаміку магнітного вихору в 2D легкоплощинному феромагнетику під впливом зовнішнього магнітного поля, що обертається в площині магнетика. Згідно з результатами чисельного моделювання під впливом змінного магнітного поля спостерігається граничний цикл в динаміці вихору, який існує в широкому діапазоні напруженостей та частот поля. Результати моделювання підтверджено аналітичним розрахунком на основі розробленого нового методу колективних змінних. Цей метод враховує внутрішні ступені вільності системи разом з координатами центра вихору.